

MICHIGAN STATE UNIVERSITY

CYCLOTRON LABORATORY

DOES THERMALIZATION OCCUR IN INTERMEDIATE ENERGY
NUCLEUS-NUCLEUS COLLISIONS

GARY D. WESTFALL

Invited talk at International Conference on Nucleus-Nucleus Collisions

Visby, Sweden



AUGUST 1985

DOES THERMALIZATION OCCUR IN INTERMEDIATE ENERGY NUCLEUS-NUCLEUS COLLISIONS?

Gary D. WESTFALL

National Superconducting Cyclotron Laboratory
Michigan State University, East Lansing, Michigan 48824-1321

Evidence for thermalization in intermediate energy nucleus-nucleus collisions is presented based on inclusive light particle and complex fragment spectra, light particle-complex fragment correlation measurements and p-p correlation results. A consistent result is obtained that nucleons and light nuclei emitted in these reactions display many characteristics of thermal systems.

1. INTRODUCTION

One of the most interesting and puzzling questions in the field of high energy nucleus-nucleus collisions concerns the question of whether thermalization is realized in reactions at incident energies ranging from 30 to 200 MeV/nucleon. Thermalization is a well known phenomenon in heavy ion collisions at energies just above the coulomb barrier where compound nuclei exhibit temperatures that are explainable in terms of Fermi gas formulations. At high energies results from sophisticated multiparticle experiments such as the those by the Plastic Ball group¹ demonstrated that a large degree of equilibration is reached for participant nucleons in high multiplicity events. A recent result by Morrissey-Benenson et. al.² casts doubt on the concept of thermalization. The purpose of this paper is to present the case in favor of thermalization in intermediate energy nucleus-nucleus collisions.

The term, thermalization, is not well defined in intermediate energy nucleus-nucleus collisions. For the purpose of this paper I will define thermalization to be signified by a common, intermediate velocity source for all observed participant particles, statistical emission of complex fragments, i.e. chemical equilibrium, and the property that these quantities vary smoothly and monotonically with incident energy. The particles under discussion here do not originate from fusion or incomplete fusion reactions or from projectile or target fragmentation processes. To study thermalization one must separate the particle spectra of interest from those that originate from target-like or projectile-like sources. The data addressed in this paper are inclusive light particle and complex fragment data from Jacak et. al.,³ systematics of light particle data and triggered light particle spectra from Hasselquist et. al.⁴

and Caskey et. al.,⁵ and light particle correlations from intermediate energy nucleus-nucleus collisions from Fox et. al.⁶

2. INCLUSIVE DATA

Light particle and complex fragment inclusive spectra have been measured by many groups over a large range of incident energies and for a large range of projectile/target systems. To be able to compare the many different systems studied one needs a method of parameterizing the data in way that will extract the essential features of the data in a compact way. Also the regions of interest must be defined such that contributions from phenomena that may have different dependence on incident energy are minimized. We have parameterized these data in terms of a single moving source model where each projectile-target-observed particle-incident energy case is fit with three parameters: velocity of the source β , temperature of the source τ , and the production cross section for the observed particles σ . The source is assumed to be described by a relativistic Boltzmann distribution and emits particles isotropically in its rest frame.

The inclusive data for p, d, and t from 30 MeV/nucleon $^{12}\text{C}+\text{Au}$ are shown in Fig. 1 along with the moving source fits shown as solid lines.⁴ An example of inclusive spectra at higher energies is shown in Fig. 2 where p, d, t, ^3He , and ^4He from 92 MeV/nucleon $^{40}\text{Ar}+\text{Au}$ are shown along with moving source fits.⁴ These data and inclusive data for light particles in general appear to be thermal in nature. They display exponential energy spectra and smooth angular distributions that are suggestive of the statistical nature of the spectra.

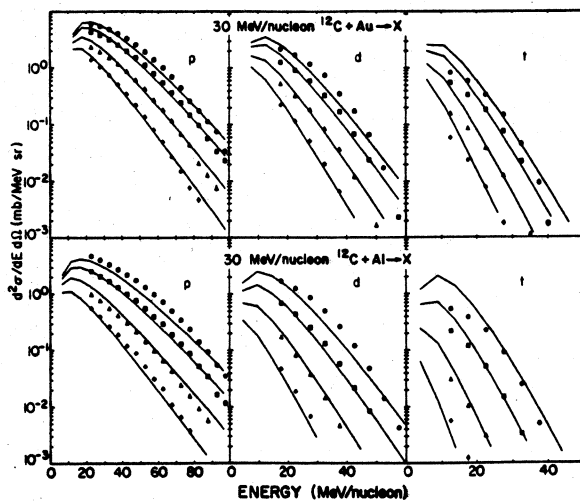


Fig. 1

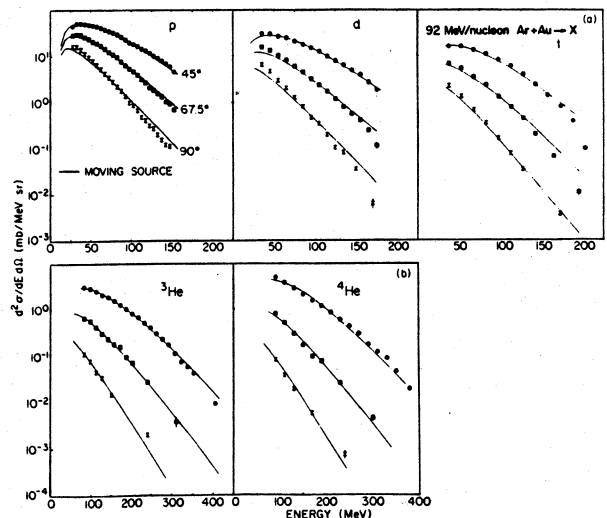
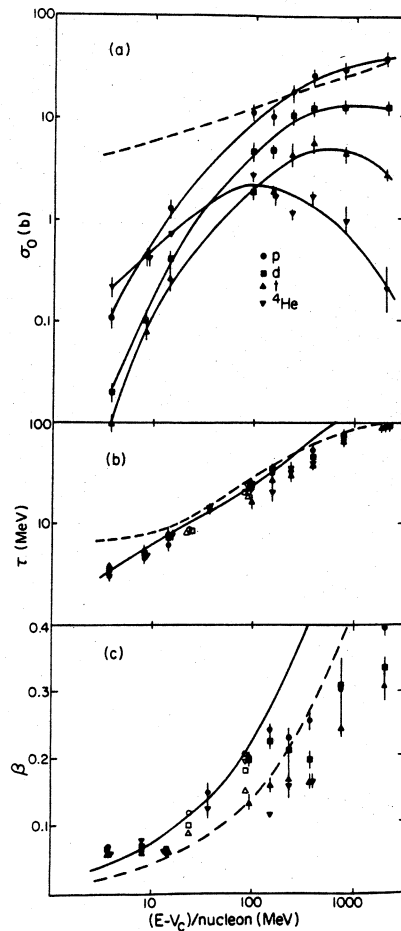


Fig. 2

We have applied the single moving source model to a large body of inclusive data for ^{12}C -, ^{16}O -, ^{20}Ne -, and ^{40}Ar -induced reactions on heavy targets. The fits include only contributions from an intermediate velocity source and explicitly exclude spectator contributions by not fitting spectra at forward angles that may contain projectile fragmentation or at low energies that may have target fragmentation contributions. The parameters σ , τ , and β for light particles emitted from an intermediate velocity source are shown in Fig. 3 as a function of energy/nucleon above the coulomb barrier.⁴ These parameters vary smoothly with incident energy suggesting that high energy nucleus-nucleus collisions at 2 GeV/nucleon may be compared to reactions at 10 MeV/nucleon. However, at low incident energies one cannot distinguish easily using this kinematic method between light particles originating from target and projectile fragmentation and thus the results at low energies must be suspect.



Inclusive light particle spectra have been explained in terms of many models that treat nuclear collisions both macroscopically and microscopically. However most of these models treat the nuclear matter in terms of nucleons only and do not include the fact that not nucleons are emitted in these reactions but that a large number of complex fragments are emitted as well. An example of complex fragment emission is shown in Fig. 4 where Be isotopes from 137

MeV/nucleon $^{40}\text{Ar} + \text{Au}$ are shown.³ It is difficult to explain the emission of a ^{10}Be at 60° at 50 MeV/nucleon simply in terms of the superposition of nucleon-nucleon scattering. Moving source parameters have been extracted from complex fragment spectra from 42, 92, and 137 MeV/nucleon $^{40}\text{Ar} + \text{Au}$ and Ca for fragments with $1 \leq A \leq 14$. These fits have been applied in such a way as to suppress contributions from target-like and projectile-like fragments. One must be careful in comparing data from other experiments such as high energy proton-induced and low energy heavy ion collisions that similar energy and angular ranges are compared. Most important is the suppression of target-like fragments that can be identified by the coulomb peak characterized by the coulomb barrier between the heavy residual target nucleus and the emitted fragment.

The temperatures extracted from moving source fits to complex fragments emitted from an intermediate velocity source are shown in Fig. 5.³ The surprising result is obtained that all the fragments ranging from protons to ^{14}N seem to have the same apparent temperature. This result suggests that all the fragments are emitted from a common, thermalized source. A possible flaw

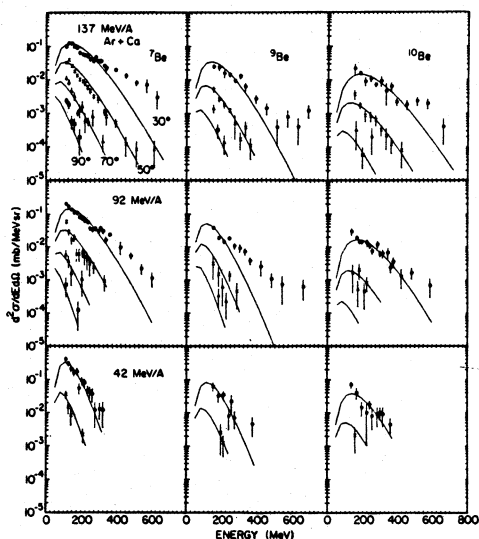


Fig. 4

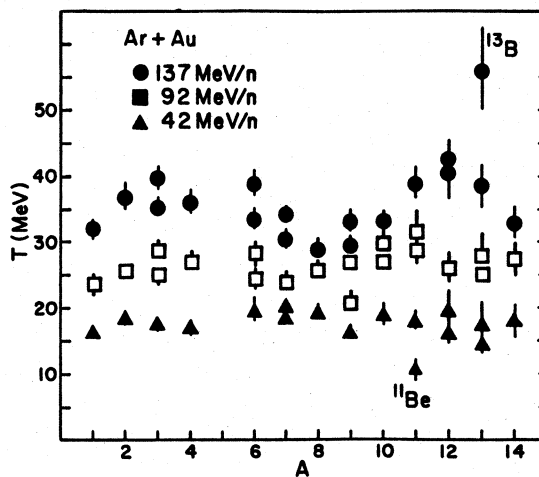


Fig. 5

is seen in this interpretation in the extracted source velocities in Fig. 6.³ The apparent source velocity decreases with increasing mass of the observed fragment suggesting that the heavier fragments do not originate from the same type of source. This decrease along with the scatter in the extracted temperatures in Fig. 5 is attributed to the high energy cutoff of the detection system which was ≈ 80 MeV/nucleon. The production cross section for these fragments are shown in Fig. 7 along with the results of a quantum statistical

calculation.³ Clearly the production of these complex fragments can be understood in terms of statistical concepts again pointing toward thermalization in terms of chemical equilibrium as well as kinetic equilibrium.

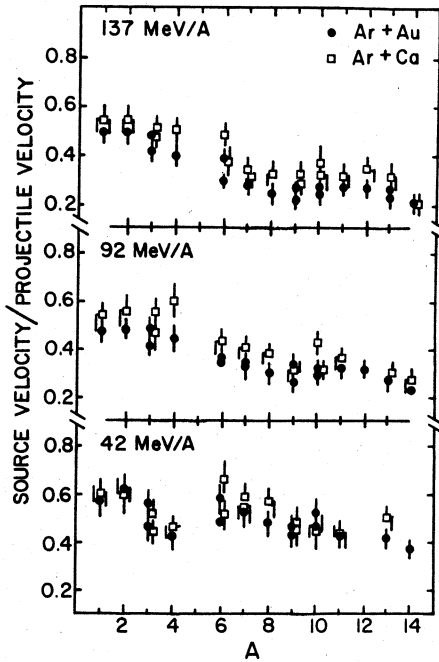


Fig. 6

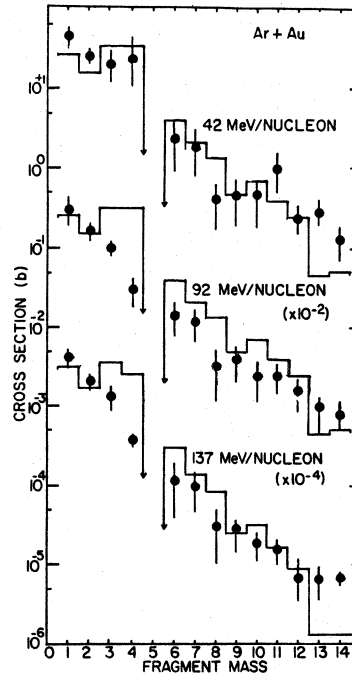


Fig. 7

3. LIGHT PARTICLE-COMPLEX FRAGMENT CORRELATIONS

The apparent thermal nature of inclusive spectra may be due to other effects besides thermalization such as the fact that averaging over many separate events that each may not be thermalized may produce spectra that on the average appear to be thermal. To remove this average over different types of events we have undertaken a series of triggered experiments to select out a given type of event topology and study the light particle spectra associated with these phenomena. The two types of events selected are events where an intermediate rapidity fragment (IRF) is emitted at large angles which should signify a violent collision and events where a projectile-like fragment (PLF) survives the collision which can be characterized as a gentle collision.

The inclusive fragment spectra ($3 \leq Z \leq 6$) for the IRF trigger at 25° are shown in Fig. 8 for 30 MeV/nucleon ^{12}C incident on Al and Au targets.⁴ The shapes of the spectra are quite similar for all the IRFs and indicate these fragments are created by similar mechanisms. Proton spectra triggered on IRFs with $3 \leq Z \leq 6$ for 30 MeV/nucleon $^{12}\text{C} + \text{Al}$ are shown in Fig. 9.⁴ The inclusive fragment spectra ($3 \leq Z \leq 7$) for the IRFs from 92 MeV/nucleon $^{40}\text{Ar} + \text{Au}$ are shown in Fig. 10. The data have been plotted as invariant cross sections as a function of the total fragment momentum. The solid lines in this figure are to guide the eye. The similarity of the shapes of the cross sections is an indication that a single reaction mechanism is responsible for the production of the various fragments.

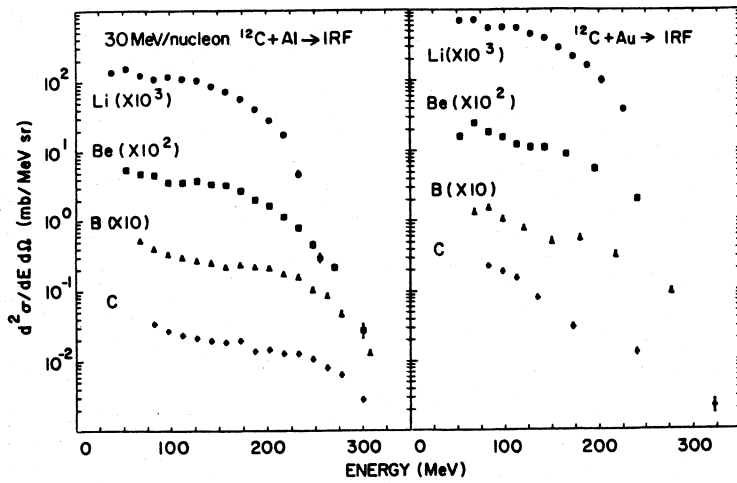


Fig. 8

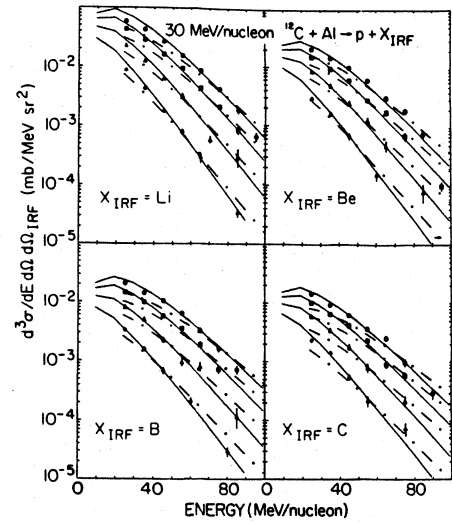


Fig. 9

Spectra for protons coincident with IRFs from 92 MeV/nucleon $^{40}\text{Ar}+\text{Au}$ are shown in Fig. 11.⁴ The inclusive light particle spectra have been included in the figures for comparison with the coincidence spectra. The coincidence spectra have the same general features as the inclusive spectra for all measured light particle - IRF combinations suggesting that these fragments have a common source.

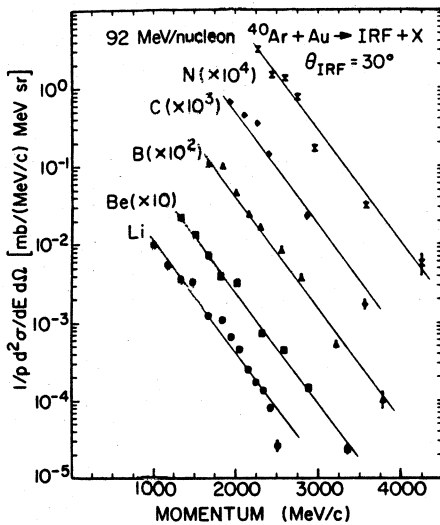


Fig. 10

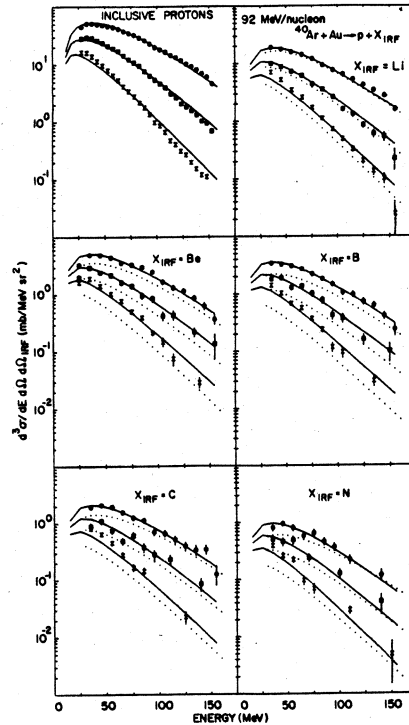


Fig. 11

The solid curves in the Figs. 9 and 11 are moving source fits to the IRF-triggered data and these fits describe the data very well and only deviate significantly for p-Li coincidences from both targets at 30 MeV/nucleon. The

extracted temperatures and velocities for the IRF triggered light particle coincidence spectra are shown in Figs. 12 and 13 as ratios of the coincidence

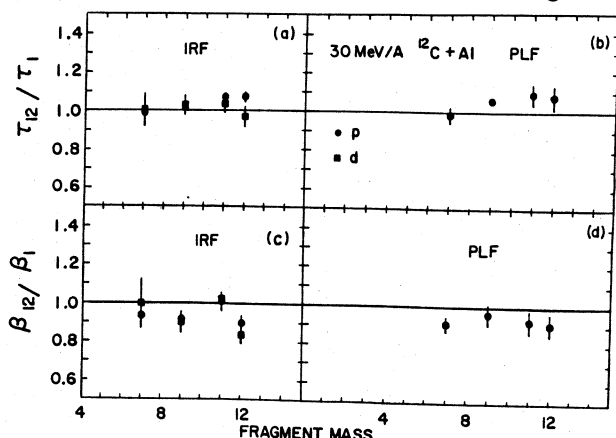


Fig. 12

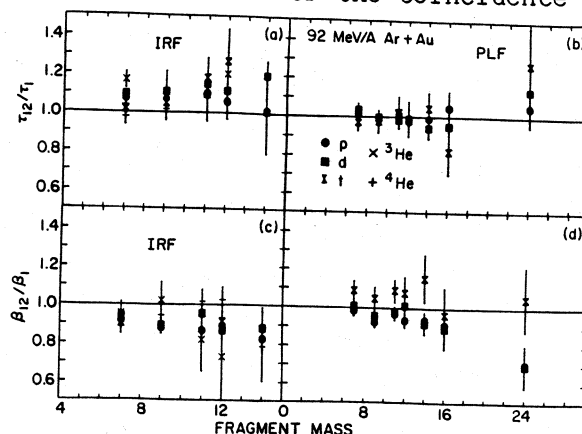


Fig. 13

values divided by the inclusive values. These ratios demonstrate that the extracted IRF-triggered temperatures tend to be about 5% higher than the inclusive temperatures at 92 MeV/nucleon but are about the same at 30 MeV/nucleon. There does not appear to be any statistically significant variation in this parameter over the range of trigger fragments measured and Figs. 12 and 13 show that the extracted coincidence spectra velocities tend to be lower than the inclusive velocities by about 10%. There are indications of a decrease in the velocity parameter with increased trigger fragment mass. There seems to be no significant dependence of the temperature and velocity parameters on the particular type of light particle measured. The apparent differences between the ^3He parameters and those of the other light isotopes may be due to the lower statistics of the ^3He spectra.

The inclusive fragment spectra ($3 \leq Z \leq 6$) for the PLF trigger are shown in Fig. 14 for 30 MeV/nucleon $^{12}\text{C} + \text{Al}$.⁴ The spectra have been plotted as a function of the ratio of the detected fragment velocity over the incident projectile velocity. One clearly sees a peak near the projectile velocity for B and C PLFs but Li and Be fragments show an exponential spectrum rather than one peaked at the beam velocity. Coincidence spectra between protons and PLFs from 30 MeV/nucleon $^{12}\text{C} + \text{Al}$ are shown in Fig. 15.⁴ The inclusive double differential cross sections for the PLF trigger at 13° are shown in Fig. 16 for 92 MeV/nucleon $^{40}\text{Ar} + \text{Au}$. Cross sections are shown for fragments with ($3 \leq Z \leq 18$) as a function of the ratio of the fragment velocity to the incident projectile velocity. The velocity distributions which most clearly show projectile fragmentation are those for O through P fragments. The Li and Be fragment velocity distributions are primarily exponential in shape with only slight shoulders to indicate the possible presence of projectile fragmentation phenomena. The B,

C, and N velocity distributions show evidence of both fragmentation and thermal emission.

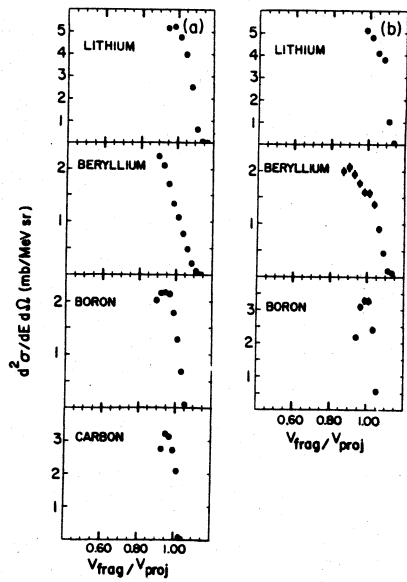


Fig. 14

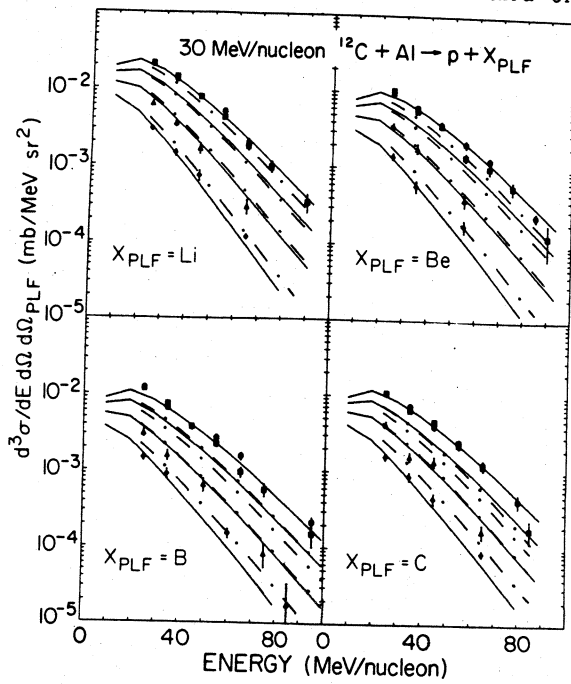


Fig. 15

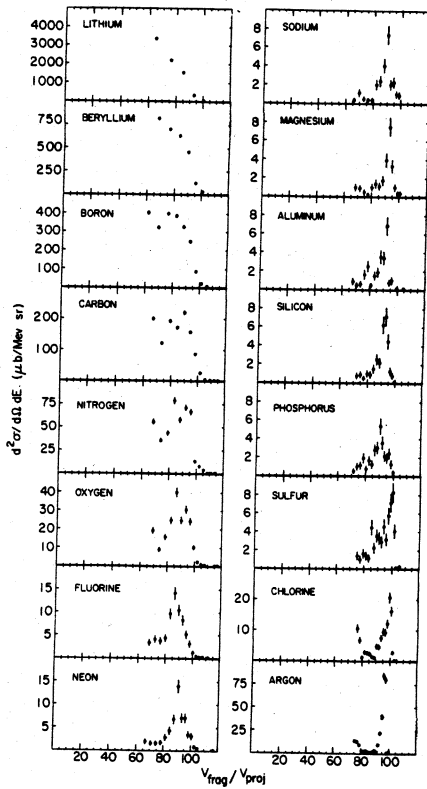


Fig. 16

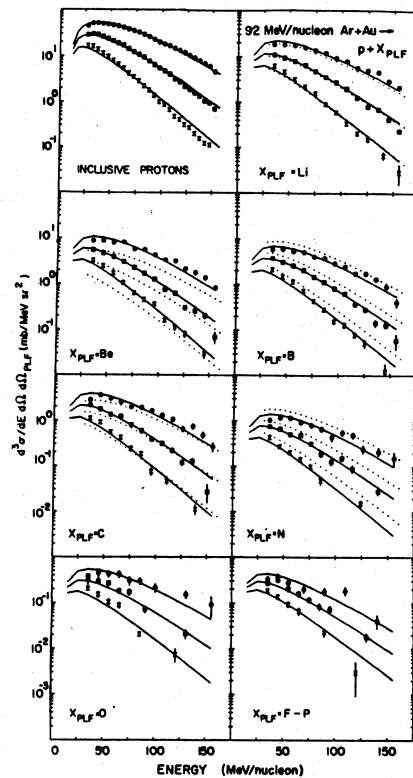


Fig. 17

The B and C spectra in Fig. 14 and the S, Cl and Ar fragment velocity distributions in Fig. 16 appear to be dominated by the few nucleon transfer

mechanism as shown by the markedly narrower widths and higher velocities relative to those of the lighter mass fragments. The apparent sudden change from fragmentation to transfer reactions at sulfur in ^{40}Ar fragmentation has been studied in reactions at 44 and 27.6 MeV/nucleon.^{7,8}

Light particle spectra for coincidences between protons and PLFs are shown in Fig. 17 for 92 MeV/nucleon $^{40}\text{Ar} + \text{Au}$.⁴ The spectra for coincident fragments with $9 \leq Z \leq 15$ have been summed together to obtain reasonable statistics. The inclusive light particle spectra have been included in this figure for comparison with the coincidence spectra. The light particle coincidence spectra for the Li through N PLF triggers appear to be very similar to the inclusive spectra. It can be seen that the proton coincidence cross sections for the O and the F through P PLF triggers have a slightly flatter angular distribution than the inclusive cross sections characteristic of a lower source velocity.

The temperatures and velocities are plotted in Figs. 12 and 13 as ratios of the coincident values to the inclusive values. Note that the parameters for spectra summed over coincidences with F through P fragments are plotted at an approximate average mass of 24. As was true for the light particle - IRF spectra, the temperature parameter shows no variation with the PLF trigger fragment mass. In addition, the PLF triggered spectra source temperatures are the same as the inclusive temperature. This constancy could reflect the fact that the PLF spectra at 13° may contain a large contribution from thermal sources. In contrast, the velocities show a clear trend toward decreasing velocities with increasing trigger fragment mass for the proton and deuteron spectra. An apparent velocity 30% below the inclusive result is obtained for the average projectile mass of $A=24$ which is consistent with the concept of emission from an excited residual target nucleus.

A similar experiment has been carried out by Caskey et. al.⁵ where the neutrons in coincidence with intermediate rapidity complex fragments were measured from the system 35 MeV/nucleon $^{14}\text{N} + \text{Ho}$. The resulting spectra for neutrons in coincidence with boron fragments at 10° are shown in Fig. 18. The circles represent neutrons spectra measured on the same side of the beam as the complex fragment and the squares represent neutrons on the opposite side. The neutrons emitted in coincidence with intermediate rapidity boron fragments show no same side-opposite side asymmetry except for the neutron detector placed directly behind the complex fragment detector which detects neutrons from sequential emission from the observed complex fragment. This constancy argues for the production of a thermalized system.

4. PROTON-PROTON CORRELATIONS

Further evidence for thermalization comes from light particle correlation measurements by Fox et. al.⁶ In this experiment the relative contribution of direct vs. thermal components was studied in reactions of 40 MeV/nucleon C + C where in-plane vs. out-of-plane correlations were studied. Light particle telescopes were placed at $(\theta, \phi) = (45^\circ, 90^\circ)$ and $(45^\circ, 180^\circ)$ and another telescope was moved from $\theta = 25^\circ$ to 120° at $\phi = 0^\circ$. No peak was observed in the ratio of in- to out-of-plane proton-proton correlations at energies and angles corresponding to quasi-elastic scattering. In Fig. 19 the ratio of the in-plane to out-of-plane p-p coincidence spectra for the case of the movable detector at 45° is shown as a function of energy in the movable telescope. The

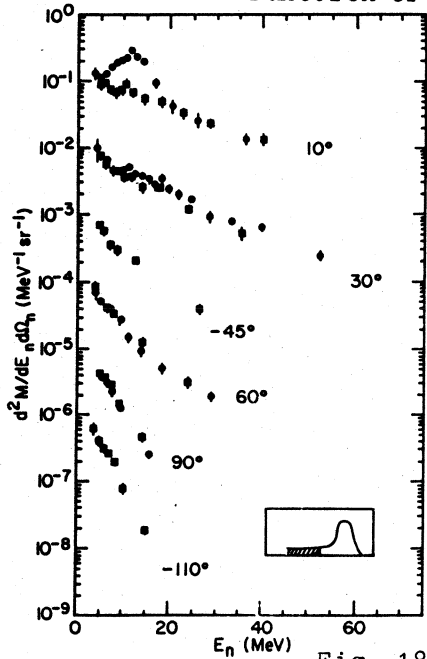


Fig. 18

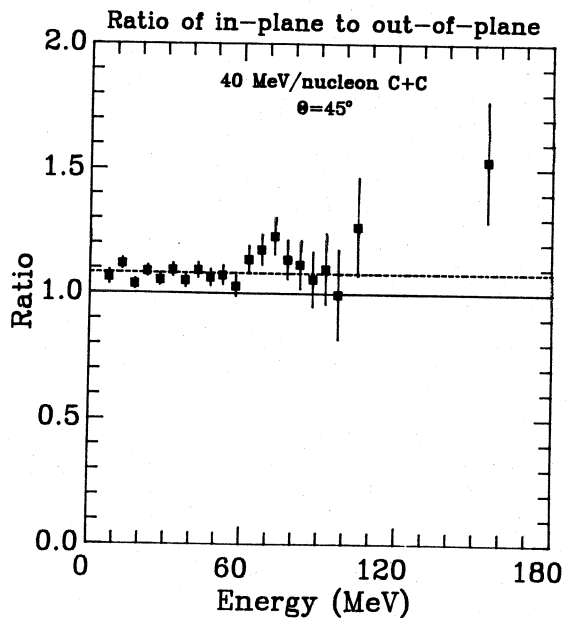


Fig. 19

correlations are integrated over all proton energies in the other two telescopes (one in-plane and one out-of-plane) covering the range from 10 to 160 MeV. This ratio is constant as a function of energy up to 60 MeV and then apparently increases although the statistics are poor. The average value for the ratio at this angle is 1.08 ± 0.01 . There is clearly no peak at 20 MeV in the ratio of in-plane to out-of-plane coincidence spectra as one would expect from free proton-proton scattering.

5. COALESCENCE MODEL

Another method of describing complex fragment spectra is the coalescence model where instead of postulating that nuclei are emitted from a system in kinetic and chemical equilibrium, one assumes that these fragments are created by the coalescence of the large number of nucleons emitted in the collision. Nucleons that are emitted within a certain radius in momentum space, p_0 , are assumed to coalesce into complex fragments. This idea leads to the result that the light nuclei can be described as simply the observed proton spectra raised

to the A^{th} power at the same energy/nucleon. This model is applied to energy spectra of complex fragments from 92 and 137 MeV/nucleon $^{40}\text{Ar} + \text{Au}$ in Fig. 20 as given by the solid lines.⁹ The overall normalization between the proton spectra to the A^{th} power and the fragment spectra gives p_0 . The values of p_0 extracted from 92 and 137 MeV/nucleon $^{40}\text{Ar} + \text{Ca}$ and Au are given in Fig. 21.⁹⁾

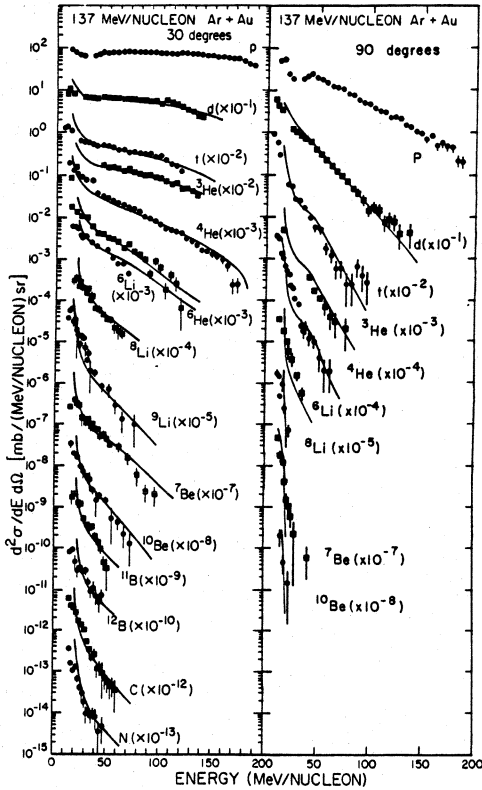


Fig. 20

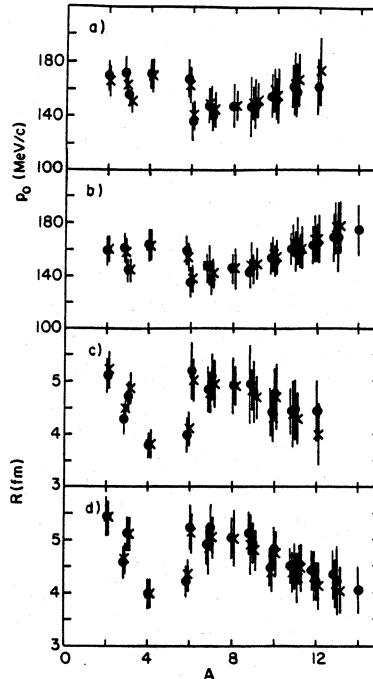


Fig. 21

One clearly sees that p_0 is independent of fragment mass and also of target mass. This constancy argues for a common emitting system and agrees with the result that the fragments display a constant temperature at a given bombarding energy. The coalescence formulation in fact can be shown to give the same dependence on fragment energy as the thermal model.

One can relate directly the apparent interaction volume radius, R , to p_0 . The extracted values for R are shown in Fig. 21 as a function of fragment mass. The apparent source size is ≈ 4.5 fm, is independent of fragment mass, and agrees with source size measurements from p-p correlations from similar sized systems at higher energies. This constant source size again argues for a common source for all fragments.

6. CONCLUSION

In conclusion the evidence for thermalization in intermediate energy nucleus-nucleus collisions can be found in inclusive light particle and complex fragment spectra where a common, thermal source has been observed for fragments

with $1 \leq A \leq 14$. These fragments also show a constant coalescence radius and apparent interaction volume radius. Correlations experiments where light particle spectra triggered on complex fragments were measured show no dramatic dependence on the trigger particles which argues that all the particles are emitted from a common source. Proton-proton correlation measurements show no direct knock-out component at 40 MeV/nucleon arguing for the dominance of thermal over single nucleon-nucleon scattering.

ACKNOWLEDGEMENTS

The author acknowledges contributions to this paper by B.V. Jacak, B.E. Hasselquist, Z.M. Koenig, and D. Fox. This work was supported by the National Science Foundation under grant no. PHY-83-12245.

REFERENCES

- 1) H.H. Gutbrod, H. Löhner, A.M. Poskanzer, T. Renner, H. Riedesel, H.G. Ritter, A. Warwick, F. Weik, and H. Wieman, Phys. Lett. 127B, 317 (1983).
- 2) D.J. Morrissey, W. Benenson, E. Kashy, B. Sherrill, A.D. Panagiotou, R.A. Blue, R.M. Ronningen, J. van der Plicht, and H. Utsumomiya, Phys. Lett. 148B, 423 (1984).
- 3) B.V. Jacak, G.D. Westfall, C.K. Gelbke, L.H. Harwood, W.G. Lynch, D.K. Scott, H. Stoecker, M.B. Tsang, and T.J.M. Symons, Phys. Rev. Lett. 51, 1846 (1983).
- 4) B.E. Hasselquist, G.M. Crawley, B.V. Jacak, Z.M. Koenig, G.D. Westfall, J.E. Yurkon, R.S. Tickle, J.P. Dufour, and T.J.M. Symons, Phys. Rev. C32, 145 (1985).
- 5) G. Caskey, A. Galonsky, B. Remington, M.B. Tsang, C.K. Gelbke, A. Kiss, F. Deak, Z. Seres, J.J. Kolata, J. Hinnefeld, and J. Kasagi, Phys. Rev. C31, 1597 (1985).
- 6) D. Fox, D.A. Cebra, Z.M. Koenig, J.J. Molitoris, P. Ugorowki, H. Stöcker, and G.D. Westfall, submitted to Phys. Rev. C, (1985).
- 7) V. Borrel, D. Guerreau, J. Galin, B. Gatty, D. Jacquet, and X. Tarrago, Z. Phys. A314, 191 (1983).
- 9) F. Rami, J.P. Coffin, G. Guillaume, B. Heusch, P. Wagner, A. Fahli, and P. Fintz, report CRN/PN.8407 (1984).
- 9) B.V. Jacak, D. Fox, and G.D. Westfall, Phys. Rev. C31, 704 (1985).